Models for pattern formation during early growth development: methods, numerics and applications

Anotida Madzvamuse

University of Sussex, UK

THE FIRST MASAMU ADVANCED STUDY INSTITUTE AND WORKSHOPS IN MATHEMATICAL SCIENCES
December 1 - 14, 2011
Livingstone, Zambia

University of Sussex

Contents

University of Sussex

Spaces and norms

Let $\Gamma_t \subset \mathbb{R}^d$ be a compact, smooth, evolving hypersurface. Taking $1 \leq p < \infty$, we define $L^p(\Gamma_t)$ Banach space:

$$L^p(\Gamma_t) = \left\{ v(\mathbf{x},t) : \int_{\Gamma_t} |v(\mathbf{x},t)|^p \, d\Gamma_t < \infty \text{ for } \mathbf{x} \in \Gamma_t,\ t \in I \right\}$$

and its corresponding norm

$$\|v(\mathbf{x},t)\|_{L^p(\Gamma_t)} = \left(\int_{\Gamma_t} |v(\mathbf{x},t)|^p \, d\Gamma_t \right)^{\frac{1}{p}}.$$

We define the following Hilbert space on $\Gamma_t,\ t \in I$.

$$H^1(\Gamma_t) = \left\{ v(\mathbf{x},t) \in L^1(\Gamma_t),\ D^{\boldsymbol{\alpha}} v \in L_1(\Gamma_t),\ |\boldsymbol{\alpha}| \leq 1 \right\},$$

where $\boldsymbol{\alpha} = (\alpha_1, \alpha_2)$, $|\boldsymbol{\alpha}| = \alpha_1 + \alpha_2$ and the distributional derivative:

$$D^{\boldsymbol{\alpha}} v = \frac{\partial^{|\boldsymbol{\alpha}|} v}{\partial^{\boldsymbol{\alpha}_1} x \, \partial^{\boldsymbol{\alpha}_2} y}.$$

US University of Sussex

Surface Derivatives: Notation

- Let $\boldsymbol{\mu}$ denote the unit outer normal to Γ_t
- Tangential Gradient on Γ_t:

$$\nabla_{\Gamma_t} u = \nabla u - (\nabla u \cdot \boldsymbol{\mu})\,\boldsymbol{\mu}$$

- The Laplace-Beltrami operator on the surface Γ_t is defined to be the tangential divergence of the tangential gradient:

$$\Delta_{\Gamma_t} u = \nabla_{\Gamma_t} \cdot \nabla_{\Gamma_t} u\,,$$

where the tangential divergence is defined as:

$$\nabla_{\Gamma_t} \cdot u = \nabla \cdot u - \sum_{i=1}^{3} \Big((\nabla u)_i \cdot \boldsymbol{\mu} \Big) \mu_i .$$

University of Sussex

Surface Integrals: Notation

Let $\boldsymbol{\beta}$ denote the flow velocity of the evolving surface.

- Transport Formula:

$$\frac{d}{dt}\int_{\Gamma_t} u = \int_{\Gamma_t} \partial^\bullet u + u\nabla_{\Gamma_t}\cdot\boldsymbol{\beta}$$

where

$$\partial^\bullet u := u_t + \boldsymbol{\beta}\cdot\nabla_{\Gamma_t} u$$

defines the material derivative following the flow.

University of Sussex

Reaction-Diffusion Systems on Evolving Surfaces

Let Γ_t be an evolving two-dimensional hypersurface in $\mathbb{R}^d$ bounding a time-dependent domain $\Omega(t)$ with unit outward pointing normal $\boldsymbol{\mu}$, then

$$
(\mathbf{P1}) \quad \begin{cases} \begin{cases} u_t + \nabla_{\Gamma_t} \cdot (\boldsymbol{\beta}\, u) = \Delta_{\Gamma_t} u + \gamma f(u,v), \\ v_t + \nabla_{\Gamma_t} \cdot (\boldsymbol{\beta}\, v) = d\Delta_{\Gamma_t} v + \gamma g(u,v), \end{cases} \quad \boldsymbol{x} \in \Gamma_t;\ t > 0, \\ \Big[\boldsymbol{\mu} \cdot \nabla_{\Gamma_t} u\Big](\boldsymbol{x},t) = \Big[\boldsymbol{\mu} \cdot \nabla_{\Gamma_t} v\Big](\boldsymbol{x},t) = 0, \quad \boldsymbol{x} \in \partial\Gamma_t,\ t > 0, \\ u(\boldsymbol{x},0) = u_0(\boldsymbol{x}), \quad \boldsymbol{x} \in \Gamma_t;\ t = 0, \\ v(\boldsymbol{x},0) = v_0(\boldsymbol{x}), \quad \boldsymbol{x} \in \Gamma_t;\ t = 0, \end{cases}
$$

where

$$\nabla_{\Gamma_t} u = \nabla u - \nabla u \cdot \boldsymbol{\mu}\boldsymbol{\mu}$$

and

$$\Delta_{\Gamma_t} u = \nabla_{\Gamma_t} u \cdot \nabla_{\Gamma_t} u.$$

University of Sussex

Variational formulation

Let $\varphi(\boldsymbol{x},t) \in H^1(\Gamma_t)$ be a test function. Multiplying the u equation of system (**P1**) by φ and integrating over Γ_t leads to

$$\int_{\Gamma_t} \gamma f(u,v)\varphi = \int_{\Gamma_t} \partial^\bullet u\varphi + u\,\varphi\nabla_{\Gamma_t}\cdot\boldsymbol{\beta} + \int_{\Gamma_t} \nabla_{\Gamma_t}u\cdot\nabla_{\Gamma_t}\varphi - \int_{\partial\Gamma_t} \varphi\nabla_{\Gamma_t}u\cdot\boldsymbol{\mu}.$$

If

- the evolving surface is closed then $\partial\Gamma_t = \emptyset$.
- well-connected but not closed (i.e. $\partial\Gamma_t \neq \emptyset$)
  - $\varphi = 0$: Dirichlet homogeneous boundary conditions
  - $\nabla_{\Gamma_t}u\cdot\boldsymbol{\mu} = 0$: homogeneous Neumann boundary conditions

University of Sussex

Variational formulation

The variational form seeks to find u and $v \in H^1(\Gamma_t)$ satisfying

$$\frac{d}{dt}\int_{\Gamma_t} u\varphi - \int_{\Gamma_t} u\partial^\bullet\varphi + \int_{\Gamma_t} \nabla_{\Gamma_t}\varphi \cdot \nabla_{\Gamma_t} u = \int_{\Gamma_t} \gamma f(u,v)\varphi,$$

$$\frac{d}{dt}\int_{\Gamma_t} v\varphi - \int_{\Gamma_t} v\partial^\bullet\varphi + d\int_{\Gamma_t} \nabla_{\Gamma_t}\varphi \cdot \nabla_{\Gamma_t} v = \int_{\Gamma_t} \gamma g(u,v)\varphi, \quad \forall\, \varphi \in H^1(\Gamma_t),$$

where

$$\partial^\bullet\varphi := \varphi_t + \boldsymbol{\beta} \cdot \nabla_{\Gamma_t}\varphi$$

defines the material derivative following the flow.

University of Sussex

Evolving surface finite element method (ESFEM)

- Barreira, R. Elliott, C.M. and Madzvamuse, A. (2011). *The surface finite element method for pattern formation on evolving biological surfaces*. Journal of Mathematical Biology. Online

University of Sussex

Concentration-driven Evolving Sphere

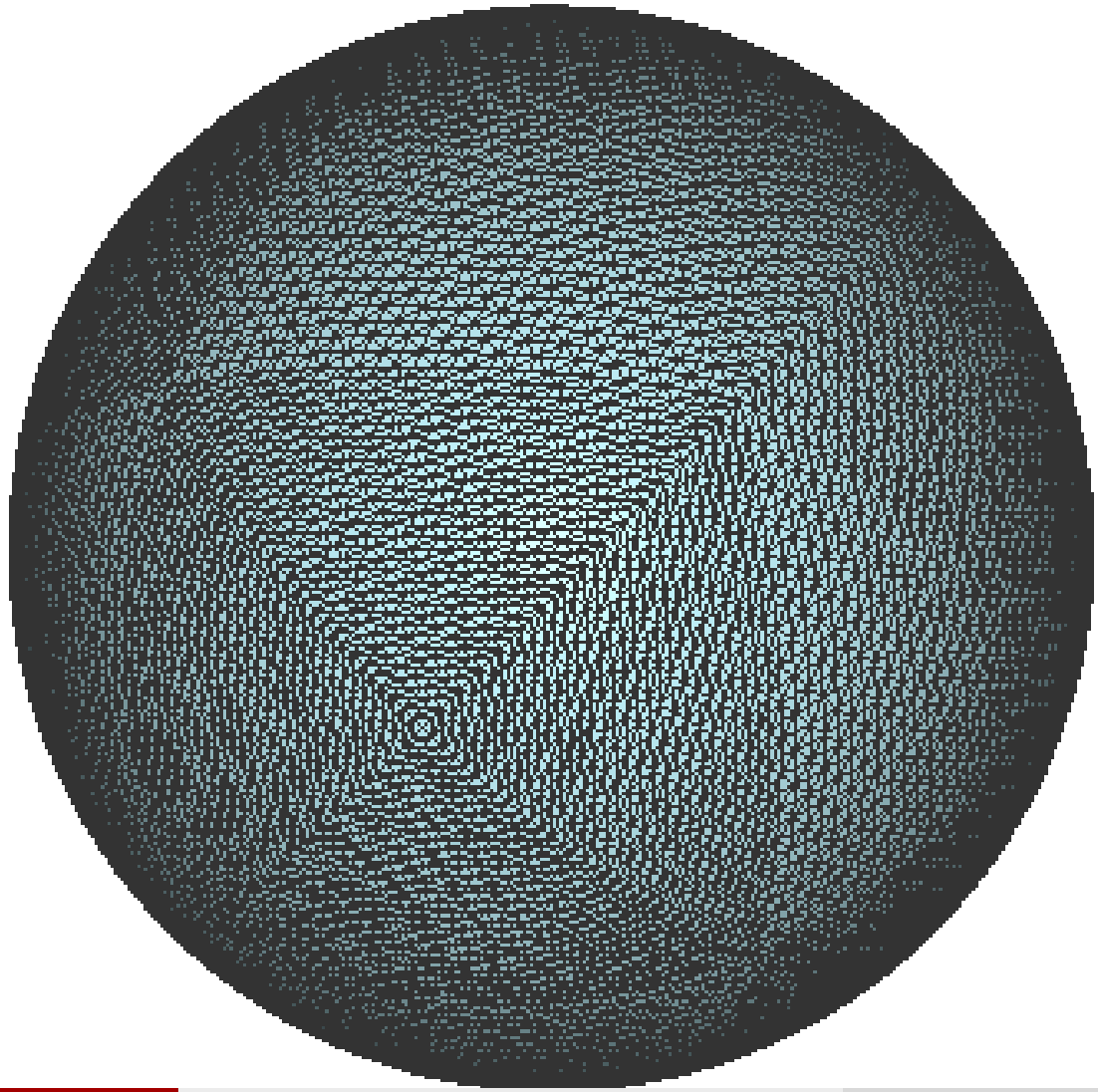

Evolving surface finite element method (ESFEM)

- We approximate Γ_t by Γ_t^h, a triangulated surface whose vertices lie on Γ_t, *i.e.* $\Gamma_t^h = \mathcal{T}_h(t) = \bigcup_k T_k(t)$, where each $T_k(t)$ is a triangle.
- We assume Γ_t^h is smooth in time.
- For each t we define a finite element space

$$S_h(t) = \left\{ \phi \in C^0(\Gamma_t^h) : \quad \phi|_{T_k} \quad \text{is linear affine for each } T_k \in \mathbb{T}_h(t) \right\}.$$

- For each $t \in [0, T_F]$ we denote by $\left\{ \chi_j(\cdot, t) \right\}_{j=1}^N$ the moving nodal basis functions and by $X_j(t)$, $j = 1, \ldots, N$ the nodes. These functions will satisfy $\chi_j(\cdot, t) \in C^0(\Gamma_t^h)$, $\chi(X_i(t), t) = \delta_{ij}$, $\chi_j(\cdot, t)\big|_{T_k}$ is linear affine, and on $T_k \in \mathbb{T}_h(t)$, $\chi_j\big|_e = \lambda_k$, for each $e \in \mathbb{T}_h(t)$ where $k = k(T_k, j)$ and $(\lambda_1, \lambda_2, \lambda_3)$ are the barycentric co-ordinates.

University of Sussex

Transport property

Proposition

On Γ_t^h, *for each* $j = 1, \ldots, N$,

$$\partial^\bullet \chi_j = 0,$$

and for each $\phi = \sum_{j=1}^N \gamma_j(t)\chi_j \in S_h(t)$ *then*

$$\dot{\phi} = \sum_{j=1}^N \dot{\gamma}_j(t)\chi_j.$$

Proof.

See Dziuk and Elliott (2007). □

Evolving surface finite element method (ESFEM)

Since the finite element approximation $u^h(\boldsymbol{x},t) \in S_h(t) \subset H^1$ and $\left\{\chi_j(\cdot,t)\right\}_{j=1}^{N}$ is the basis of $S_h(t)$ we know that for each $t \in \left[0, T_F\right]$ there exist $\boldsymbol{U} = \left\{U_1(t), \ldots, U_N(t)\right\}$ such that

$$u^h(\boldsymbol{x},t) = \sum_{j=1}^{N} U_j(t)\chi_j(\boldsymbol{x},t).$$

University of Sussex

Evolving surface finite element method (ESFEM)

Substituting $u^h(\boldsymbol{x},t)$ (and similarly $v^h(\boldsymbol{x},t)$) we obtain

$$\frac{d}{dt}\int_{\Gamma_t^h}\sum_{j=1}^{N}U_j(t)\chi_j\varphi+\int_{\Gamma_t^h}\sum_{j=1}^{N}U_j\nabla_{\Gamma_t}\chi_j\cdot\nabla_{\Gamma_t}\varphi=\int_{\Gamma_t^h}\gamma f(u^h,v^h)\varphi,$$

$$\frac{d}{dt}\int_{\Gamma_t^h}\sum_{j=1}^{N}V_j(t)\chi_j\varphi+d\int_{\Gamma_t^h}\sum_{j=1}^{N}V_j\nabla_{\Gamma_t}\chi_j\cdot\nabla_{\Gamma_t}\varphi=\int_{\Gamma_t^h}\gamma g(u^h,v^h)\varphi,$$

for all $\varphi\in S_h(t)$ and taking $\varphi=\chi_k, k=1,\dots,N$ we obtain the system of nonlinear ODEs

$$\frac{d}{dt}\left(M(t)\boldsymbol{U}\right)+K(t)\boldsymbol{U}=\gamma\boldsymbol{F}(t),$$

$$\frac{d}{dt}\left(M(t)\boldsymbol{V}\right)+dK(t)\boldsymbol{V}=\gamma\boldsymbol{G}(t).$$

University of Sussex

Evolving surface finite element method (ESFEM)

- Evolving mass matrix

$$M(t)_{jk} = \int_{\Gamma_t^h} \chi_j \chi_k$$

- Evolving stiffness matrix

$$K(t)_{jk} = \int_{\Gamma_t^h} \nabla_{\Gamma_t} \chi_j \cdot \nabla_{\Gamma_t} \chi_k$$

- Evolving force vectors

$$\boldsymbol{F}(t) = \int_{\Gamma_t^h} f(u^h, v^h) \chi_j$$

$$\boldsymbol{G}(t) = \int_{\Gamma_t^h} g(u^h, v^h) \chi_j$$

University of Sussex

Time discretization

Applying the second order semi-implicit finite differentiation formula (2-SBDF) [Madzvamuse, 2005] we obtain the following fully discrete algorithm:

1. Given $\boldsymbol{U}^0, \boldsymbol{V}^0 \in S_h^0$ and $\boldsymbol{U}^1, \boldsymbol{V}^1 \in S_h^1$.
2. For $n = 1, \ldots, n_T$, solve the linear system

$$\Big(3M^{n+1} + 2\Delta t K^{n+1}\Big)\boldsymbol{U}^{n+1} = 4M^n\boldsymbol{U}^n - M^{n-1}\boldsymbol{U}^{n-1} + 2\Delta t\Big(2\gamma\boldsymbol{F}^n - \gamma\boldsymbol{F}^{n-1}\Big),$$

$$\Big(3M^{n+1} + 2\Delta t K^{n+1}\Big)\boldsymbol{V}^{n+1} = 4M^n\boldsymbol{V}^n - K^{n-1}\boldsymbol{V}^{n-1} + 2\Delta t\Big(2\gamma\boldsymbol{G}^n - \gamma\boldsymbol{G}^{n-1}\Big).$$

University of Sussex

Radially projected finite elements

- Tuncer, N. Meir, A.J. and Madzvamuse, A. *Radially Projected Finite Elements for Reaction-Diffusion Systems on Fixed Spheroidal Domains*, In preparation

University of Sussex

Schnakenberg reaction kinetics (1979)

This is one of the simplest reaction kinetic models. It is derived from a series of hypothetical tri–molecular autocatalytic reactions proposed by Schnakenberg (1979):

$$f(u,v) = 0.1 - u + u^2 v,$$

$$g(u,v) = 0.9 - u^2 v.$$

University of Sussex

Numerical solutions on fixed spheres

Initial conditions:

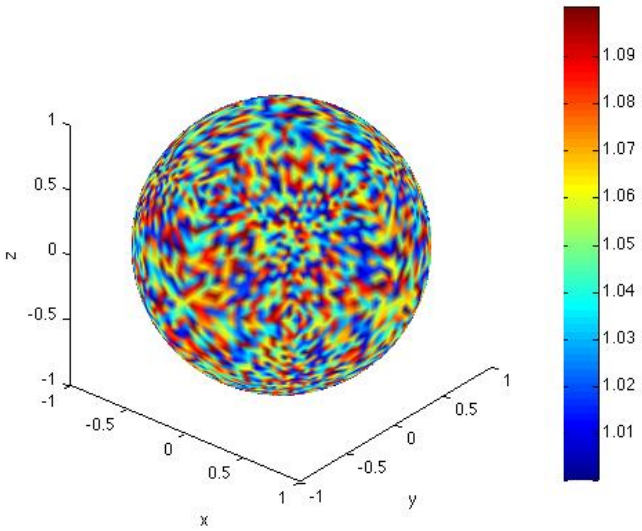

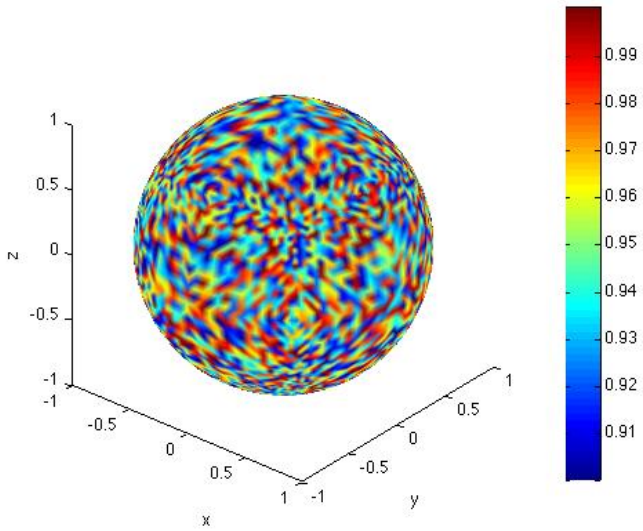

University of Sussex

Numerical solutions on fixed spheres

a	b	d	γ	Time step	#iterations	Mesh size	#elements
0.1	0.9	10	500	0.005	2000	0.0882	12288

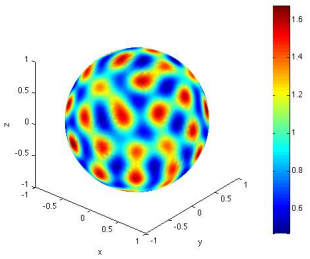

(c) $u\,, t = 1$

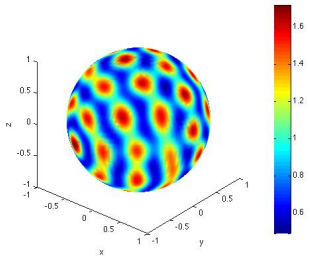

(d) $u\,, t = 2$

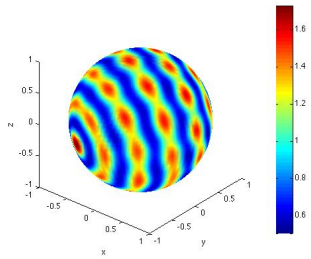

(e) $u\,, t = 3$

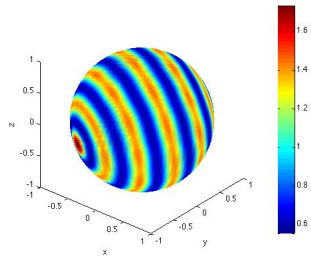

(f) $u\,, t = 5$

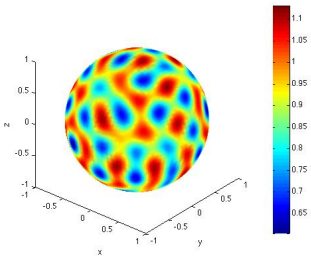

(g) $v\,, t = 1$

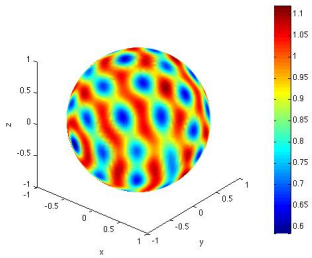

(h) $v\,, t = 2$

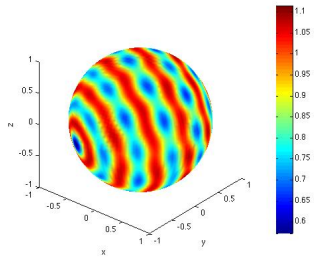

(i) $v\,, t = 3$

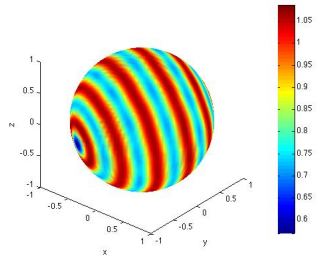

(j) $v\,, t = 5$

University of Sussex

$\gamma = 10, 29, 60, 200, 500$

a	b	d	γ	Time step	#iterations	Mesh size	#elements
0.1	0.9	10	500	0.005	2000	0.0882	12288

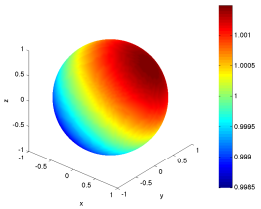

(k) $\gamma = 10$

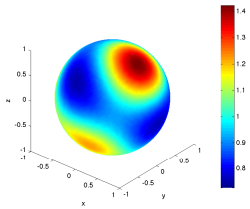

(l) $\gamma = 29$

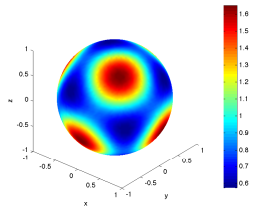

(m) $\gamma = 60$

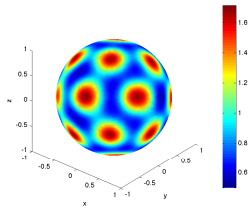

(n) $\gamma = 200$

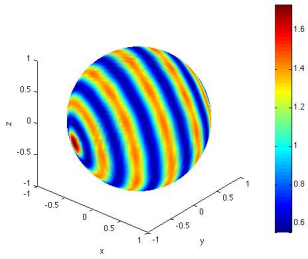

(o) $\gamma = 500$

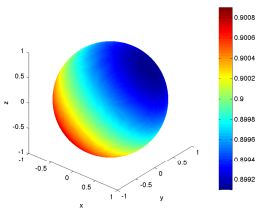

(p) $\gamma = 10$

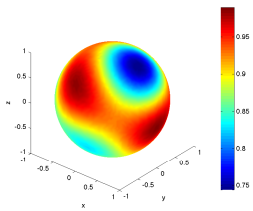

(q) $\gamma = 29$

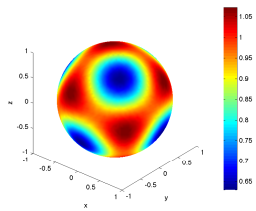

(r) $\gamma = 60$

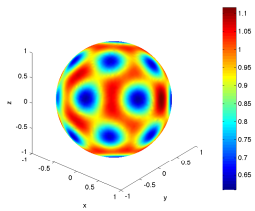

(s) $\gamma = 200$

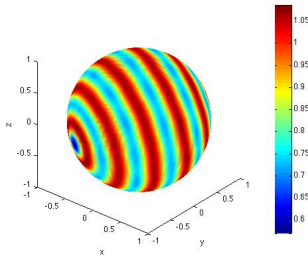

(t) $\gamma = 500$

University of Sussex

Numerical solutions on fixed cylindrical surfaces

- Let Γ be a cylinder with spherical caps.
- Initial condition is taken to be small random perturbations around the uniform steady state

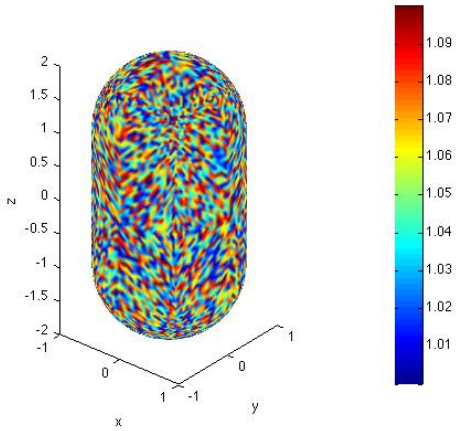

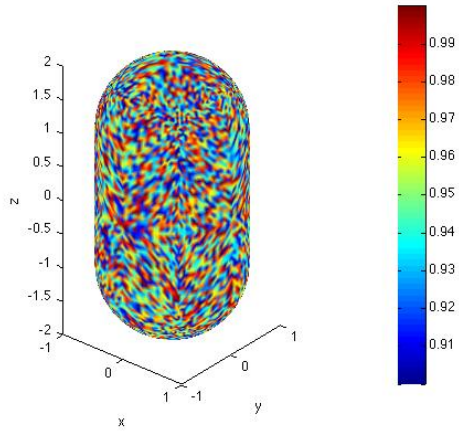

University of Sussex

Numerical solutions on fixed cylindrical surfaces

a	b	d	γ	Time step	#iterations	Mesh size	#elements
0.1	0.9	10	500	0.0025	4000	0.0882	20480

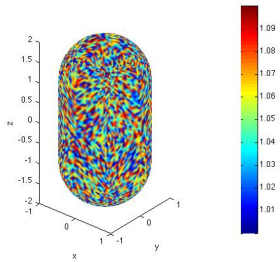

(w) u , $t = 0$

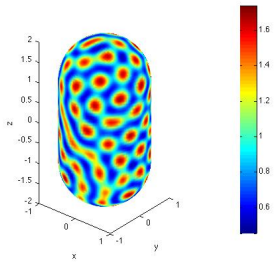

(x) u , $t = 1$

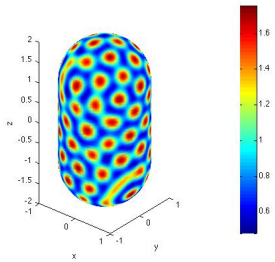

(y) u , $t = 3$

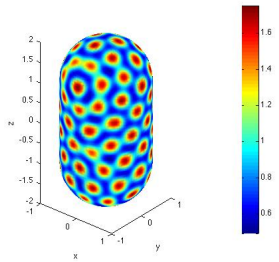

(z) u , $t = 5$

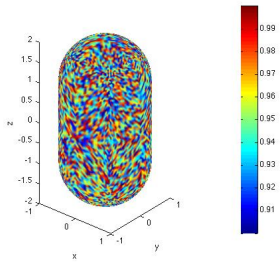

() v , $t = 0$

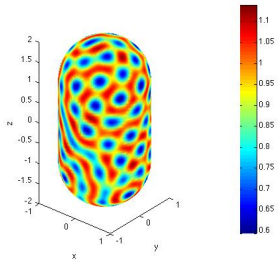

() v , $t = 1$

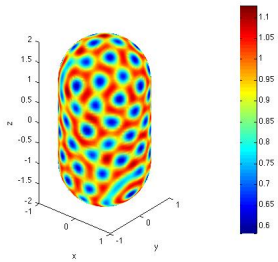

() v , $t = 3$

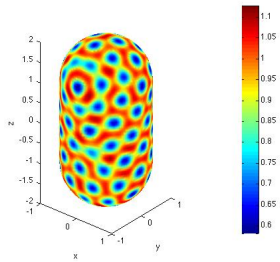

() v , $t = 5$

University of Sussex

Numerical on fixed cylindrical surfaces

a	b	d	γ	Time step	Mesh size	#elements
0.1	0.9	10	114	0.005	0.1948	11264

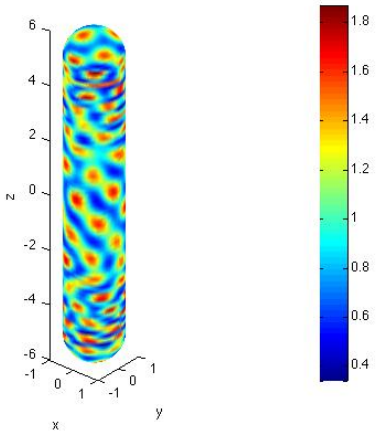

() $t = 2.5$

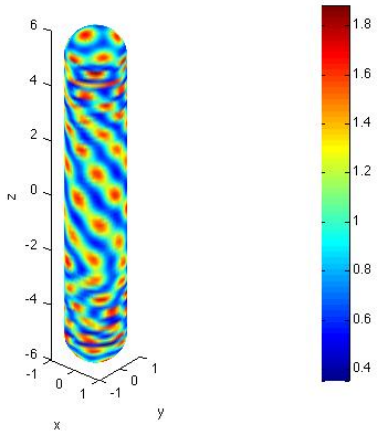

() $t = 5$

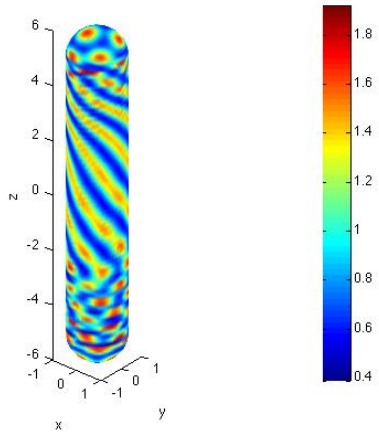

() $t = 10$

University of Sussex

Numerical solutions on fixed cylindrical surfaces

a	b	d	γ	Time step	Mesh size	#elements
0.1	0.9	10	114	0.005	0.1948	11264

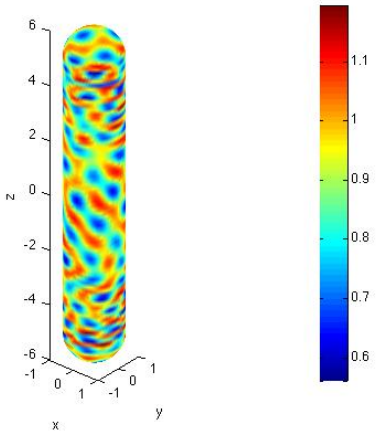

() $t = 2.5$

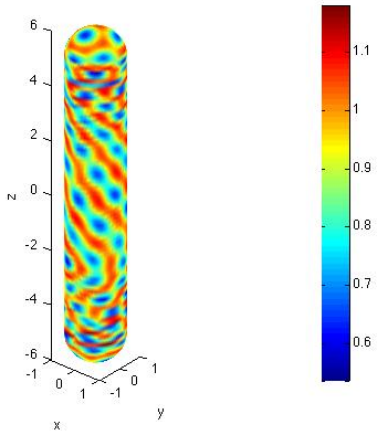

() $t = 5$

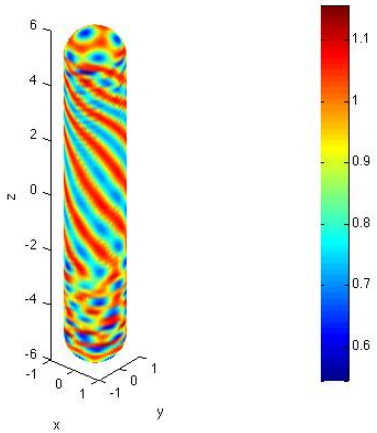

() $t = 10$

University of Sussex

Uniform isotropic logistic growth function

Consider and unit sphere evolving according to:

$$\boldsymbol{x}(t) = \boldsymbol{X}_0 \rho(t)$$

where the logistic growth function $\rho(t)$ defined by

$$\rho(t) = \frac{e^{rt}}{1 + \frac{1}{K}\left(e^{rt} - 1\right)},$$

where $r > 0$ and $K > 1$. Here r is the growth rate of the surface and K is the limiting final fixed size of the radius.

University of Sussex

Uniform isotropic logistic growth function: $t = 10,\ 30,\ 50$ and $t = 70$.

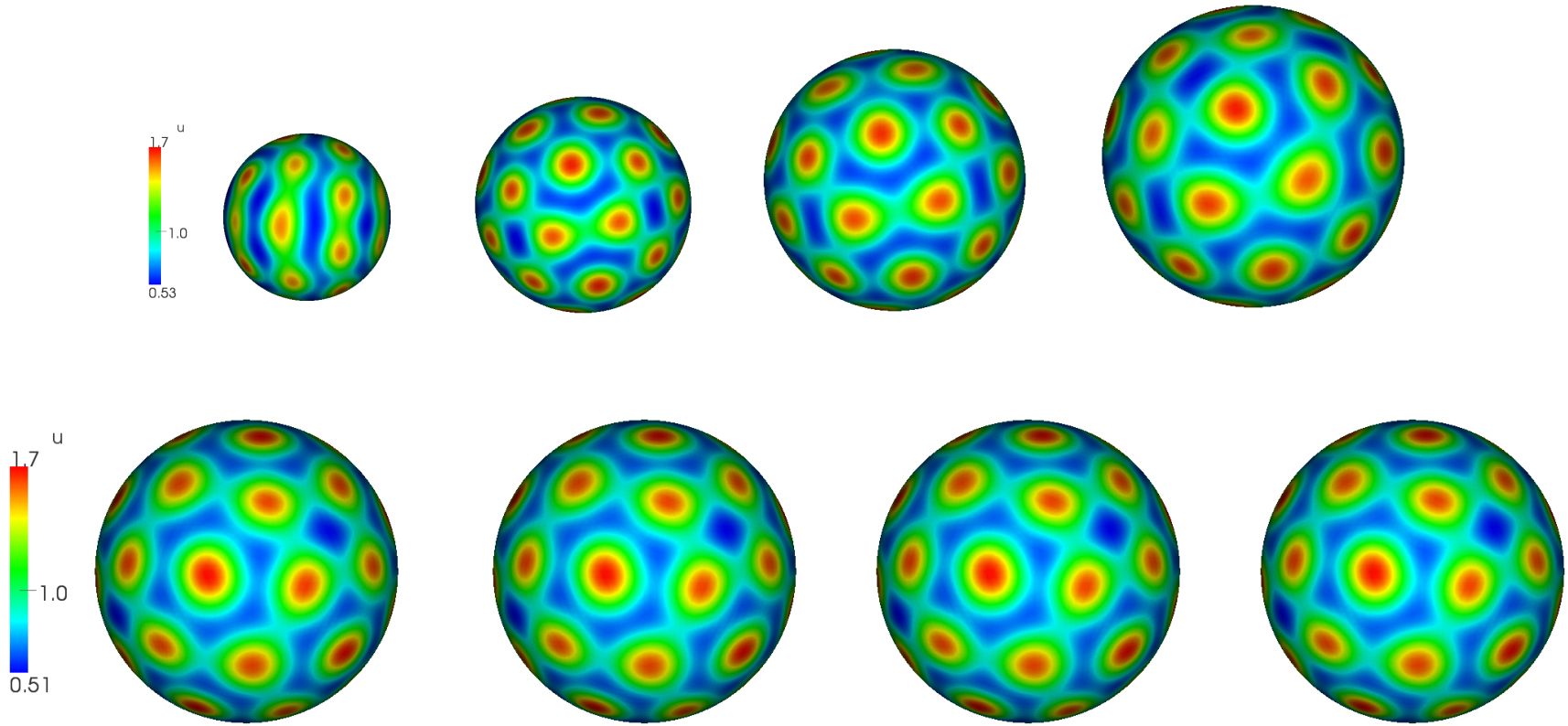

University of Sussex

Anisotropic growth: Evolving cylinder

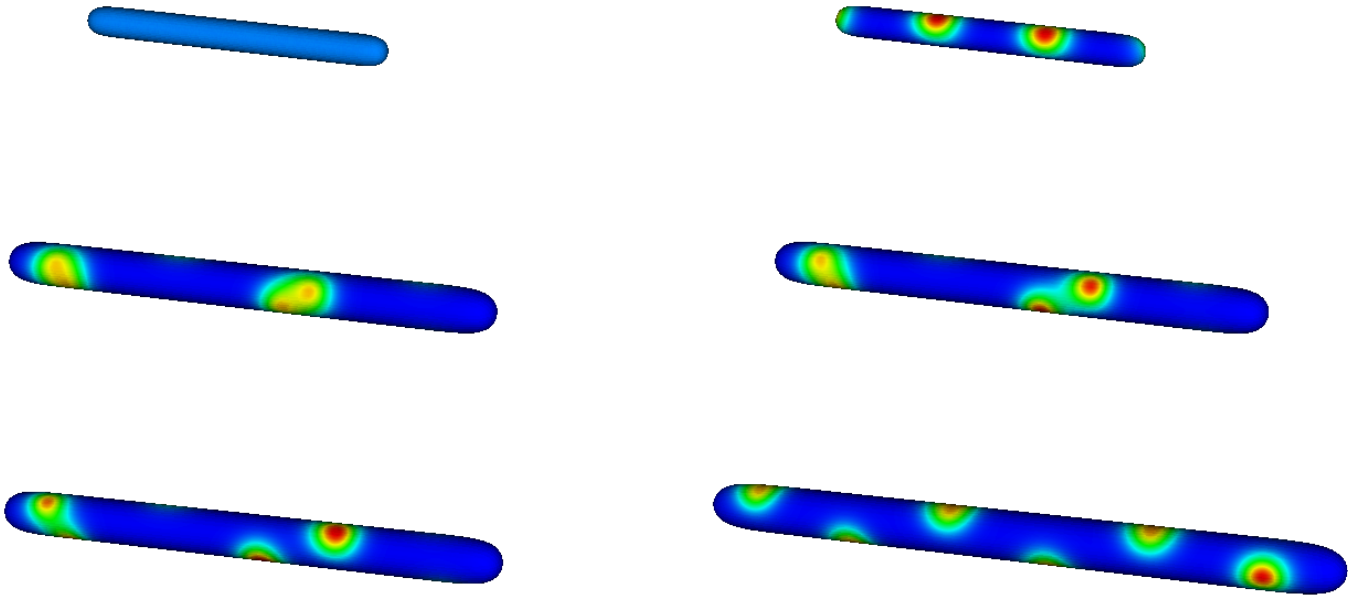

University of Sussex

Concentration-driven Evolving Surfaces

$$\boldsymbol{\beta} := \frac{\partial \boldsymbol{x}}{\partial t} = \boldsymbol{Ch}\Big(u, v, \boldsymbol{\mu}, \kappa\Big) + \epsilon \frac{\partial^2 \boldsymbol{x}}{\partial s^2}, \qquad s \in \partial\Gamma_t.$$

University of Sussex

Concentration-driven Evolving Surfaces

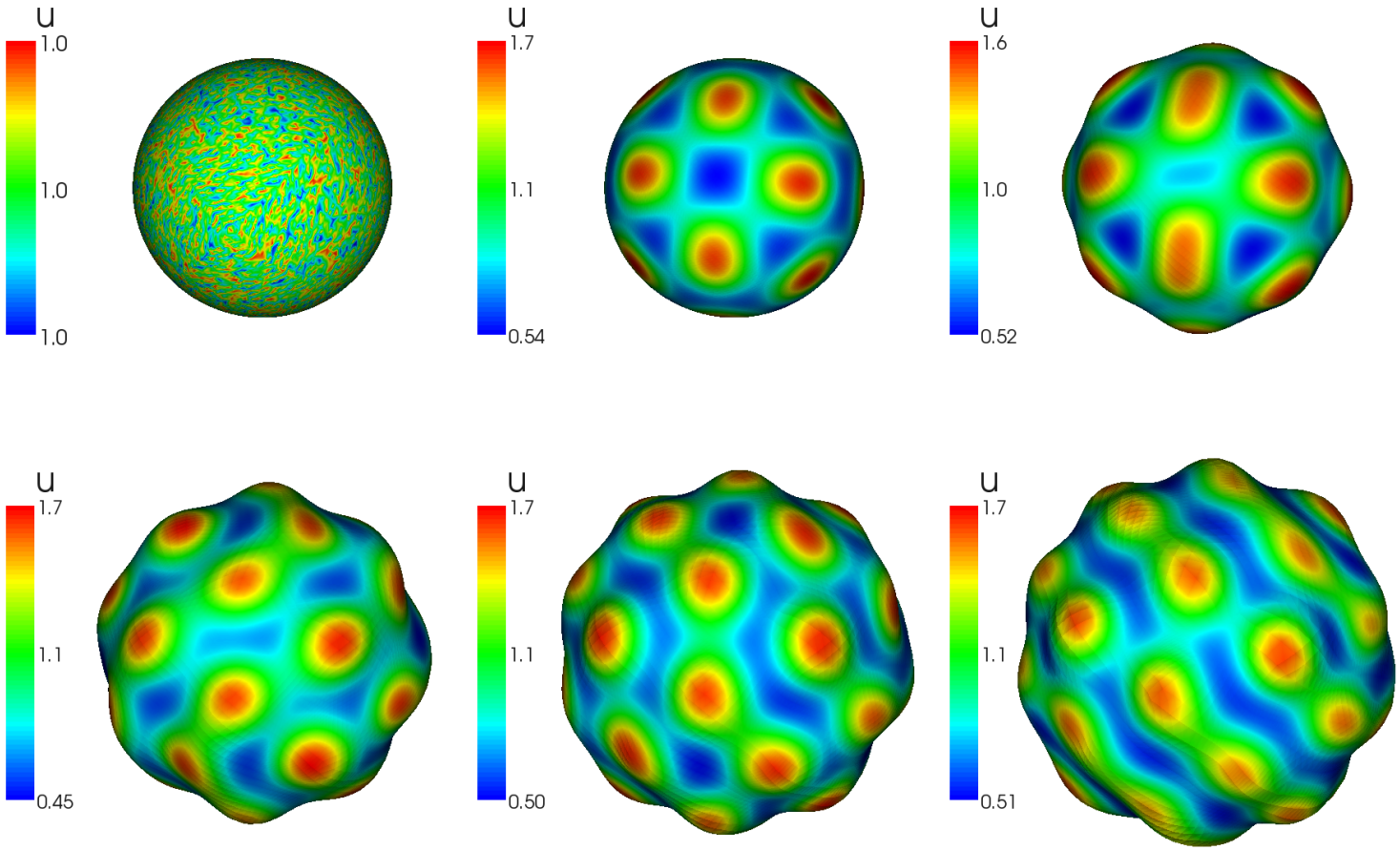

University of Sussex

Concentration-driven Evolving Sphere

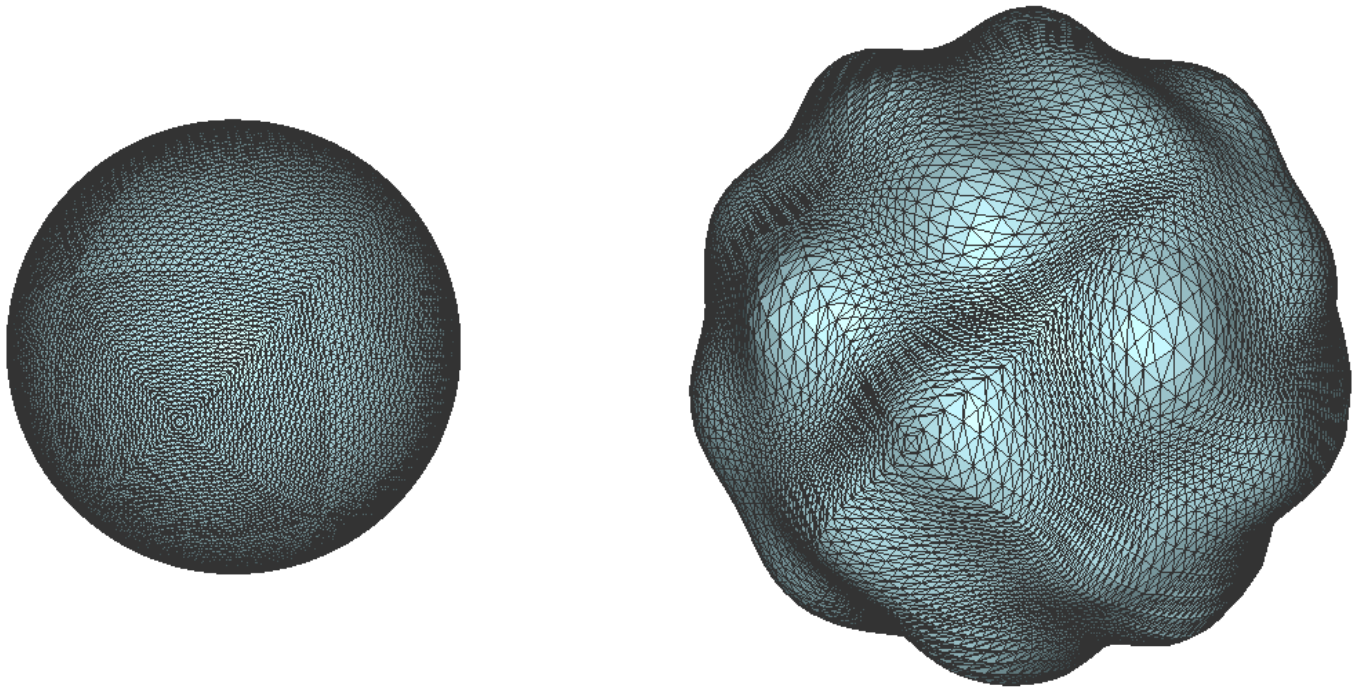

University of Sussex

A model for parr mark pattern formation during the early development of Amago trout

- Chandrashekar, V. Sekimura T. Eamonn, G.A. Maini, P.K. and Madzvamuse, A. (2011). *A model for parr mark pattern formation during the early development of Amago trout*. Physica Rev. E. Online.

University of Sussex

From juvenile to adulthood

() ∼30 days left

() ∼30 days right

() ∼60 days left

() ∼60 days right

University of Sussex

From juvenile to adulthood

() ~90 days left

() ~90 days right

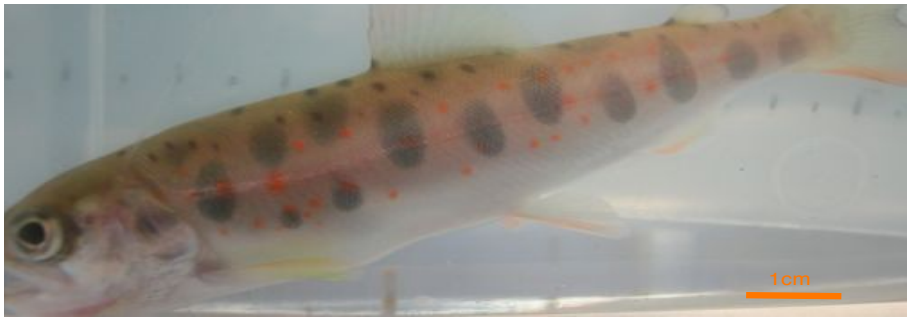

() ~160 days left

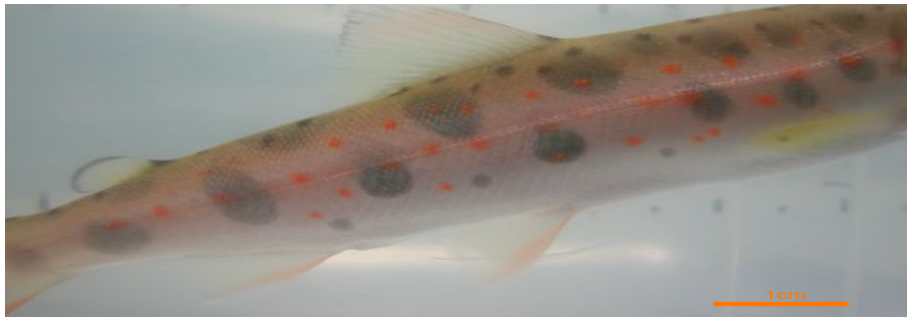

() ~160 days right

University of Sussex

From juvenile to adulthood

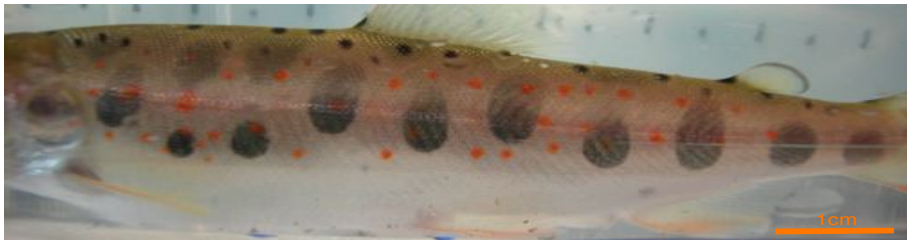

1cm

() ∼200 days left

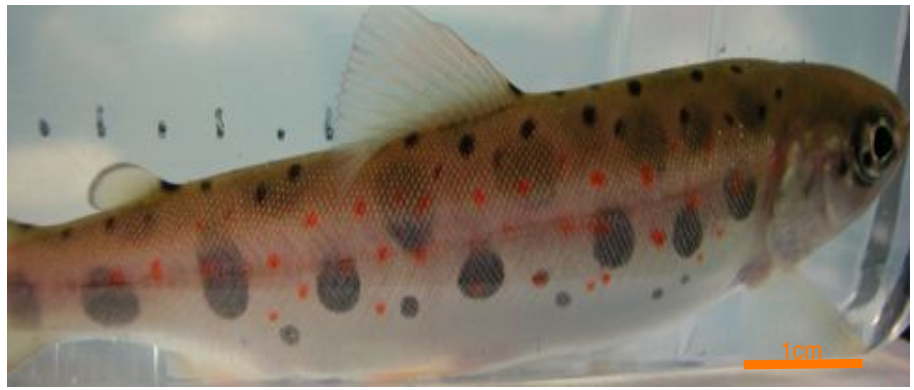

() ∼200 days right

University of Sussex

Biological observations

Stage 1: (Length: 2-4 cm, soon after hatching) No visible parr marks. During this period the Amago's diet consists only of yolk from its egg.

Stage 2: (Length: 4-6 cm, $\sim$1 month after hatching) The first stage of parr mark formation occurs. Around 5 stripe-like parr marks appear on each side of the fish towards the top (dorsal) portion. The stripes are oriented perpendicular to the head-tail axis. By this time the fish has completely consumed its egg yolk and has started to eat food from the environment.

University of Sussex

Biological observations

Stage 3: (Length: 6-8 cm, 2 to 3 months) By this stage of development the fish has grown to around 3 to 4 times its original size. Between 5 and 7 parr marks are visible on each side of the fish towards the top portion. The parr marks are still primarily oriented perpendicular to the head-tail axis, however on wider portions of the fish a zigzag orientation is somewhat evident.

Stage 4: (Length: 8-12 cm, 3 to 7 months) A new line of parr marks appears on the top of the fish. The visible pattern consists of 3 or 4 rows (parallel to the head-tail axis) of elliptical parr marks with 7 to 11 parr marks in each row. The parr marks are all located towards the top portion of the fish and are distributed in a regular zigzag orientation (checkerboard pattern). This configuration persists into maturity.

US University of Sussex

From juvenile to adulthood

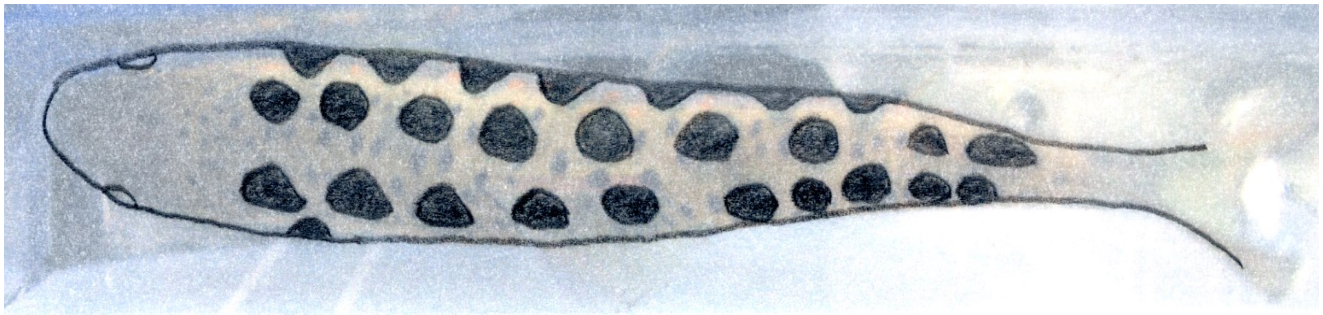

University of Sussex

Fitting a growth function to the experimental data

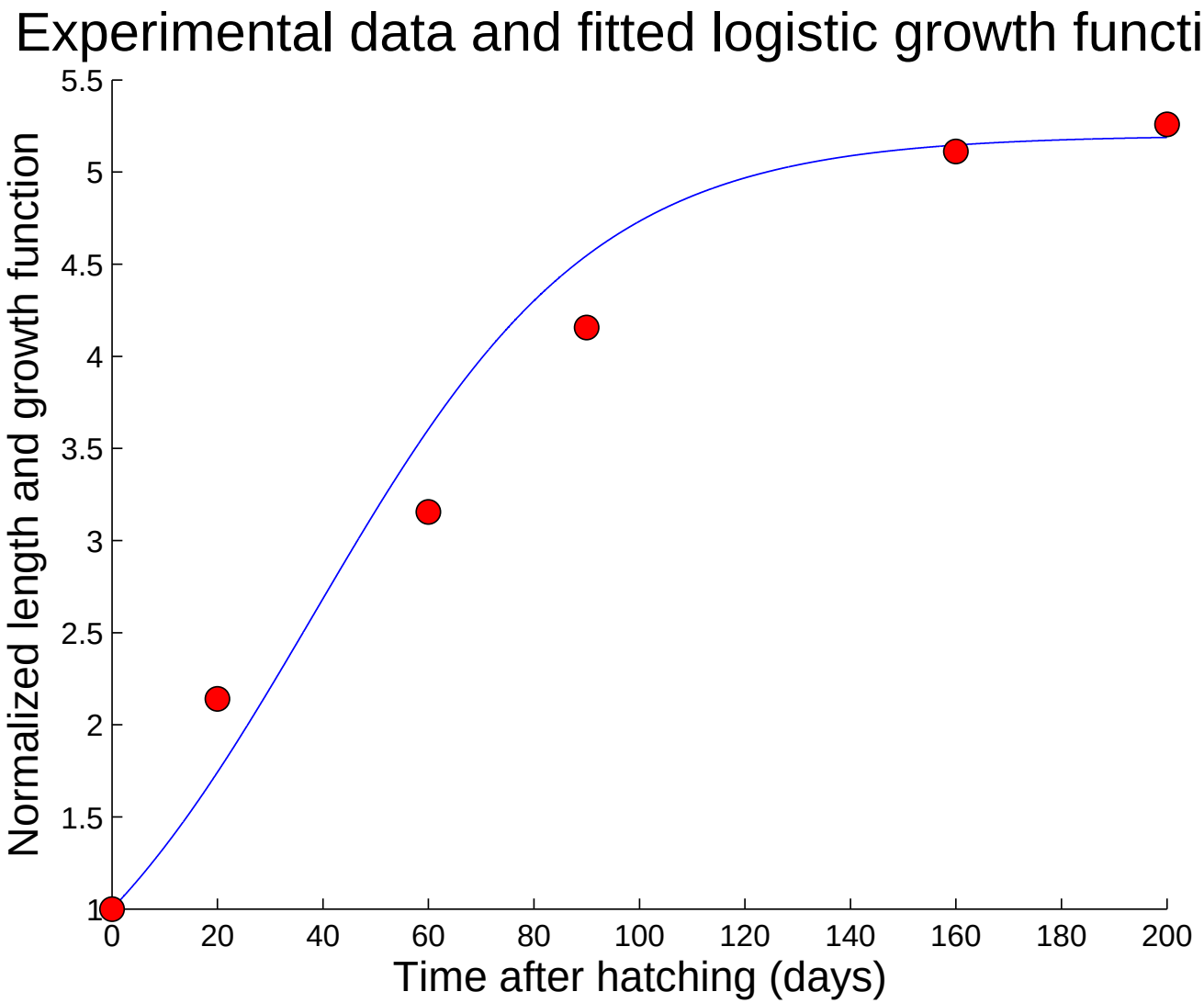

University of Sussex

Fitting a growth function to the experimental data

- We consider the *logistic growth function*.
- The fish's growth is approximately exponential initially, linear at intermediate stages and finally saturates as the organism approaches a limiting surface size, defined by:

$$\rho(t) = \frac{e^{rt}}{1 + \frac{1}{m}\left(e^{rt} - 1\right)} \qquad \text{for } t \in [0, T]\,. \tag{1}$$

- The function $\rho(t)$ represents the time dependent dilation that describes the uniform level of enlargement from the initial size of the fish to the current size of the fish.
- $m = 5.2$ to represent the nondimensional limiting surface size of the Amago fish and $r = 7.5 \times 10^{-5}$ the linear logistic growth rate.
- Take a computational time interval of $[0, 10^5]$: 1 day : 500 in computational time.

University of Sussex

Boundary conditions for the patterned surface

- The absence of any pattern on the underside of the fish at all stages of development
- Recent experimental studies of the zebrafish have shown that some of the chromatophores (pigment cells) involved in the skin patterning of the fish originate from the neural crest on the dorsal (top) side of the fish and migrate to other parts of the fish in the embryonic state
- We assume the domain on which the chromatophores are present is limited and that these chromatophores are then triggered to produce pattern by the RDSs which is posed on the same domain
- From a modelling perspective, this is equivalent to assuming that there is no-flux of morphogens between the patterned and unpatterned regions

University of Sussex

Modelling the patterned surface

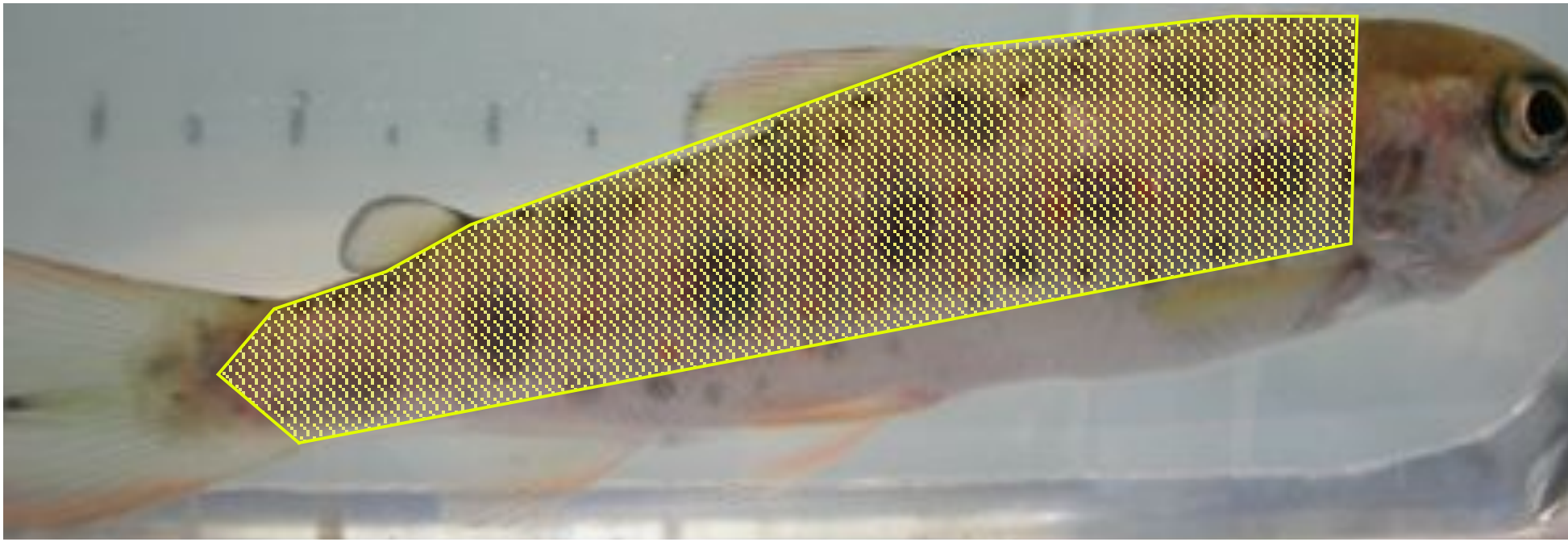

University of Sussex

Curvature considerations of the patterned surface

- Model the surface by a *planar* polygonal domain, approximating the shape of the patterned region.
- From inspection of the outline of the patterned region, a piecewise linear boundary with 6 vertices on each side provides a good approximation to the curved boundary of the patterned region.
- From inspection of the fish shape, a natural surface to investigate is a portion of a growing *elliptic cylinder*. The cylindrical surfaces we consider are defined by a mapping that maps points from a time-independent planar reference configuration, which we take to be the coordinates of the initial planar triangulation to the growing surface of an elliptic cylinder (Arbitrary Lagrangian-Eulerian Formulation).

University of Sussex

Approximation with a cylindrical surface

$$\boldsymbol{x}(t) := \rho(t) \begin{pmatrix} a\cos\left(\pi\xi_1/0.45\right) \\ b\sin\left(\pi\xi_1/0.45\right) \\ \xi_2 \end{pmatrix}$$

where ξ_1 and ξ_2 are the y (width) and x (length) coordinates of the planar approximation and $\rho(t)$ is the logistic growth function defined by

$$\rho(t) = \frac{e^{rt}}{1 + \frac{1}{m}\left(e^{rt} - 1\right)} \qquad \text{for } t \in [0, T],$$

where $m = 5.2$ and $r = 7.5 \times 10^{-5}$.

University of Sussex

Computational domain

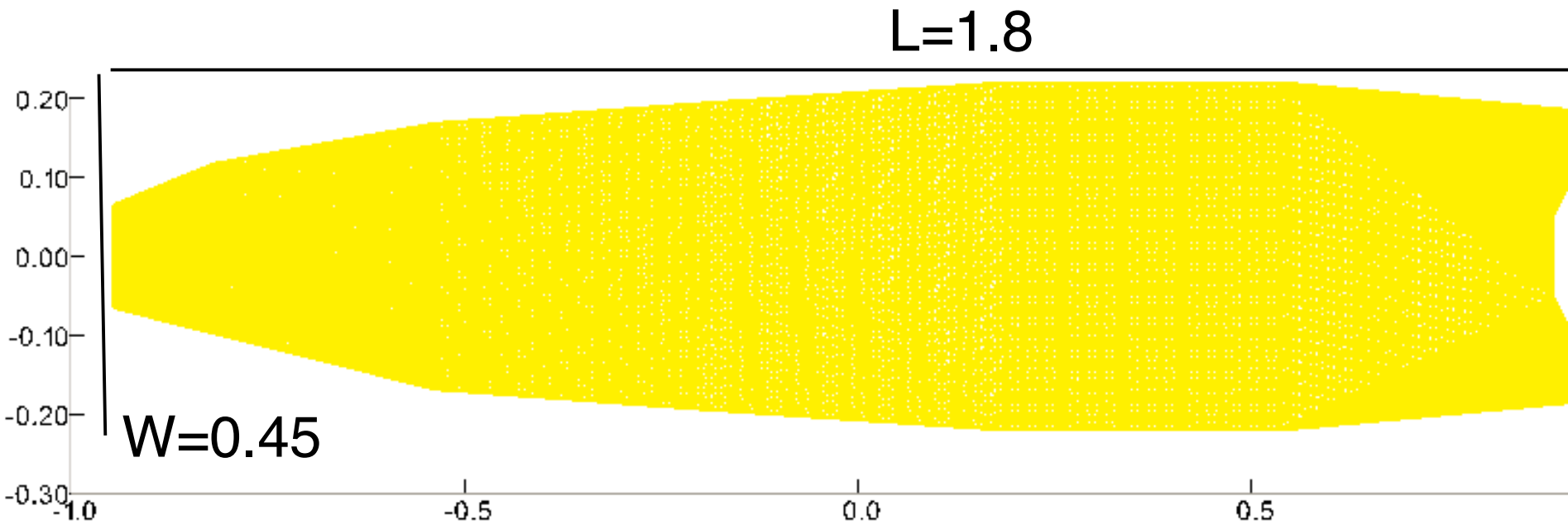

University of Sussex

Computational surface

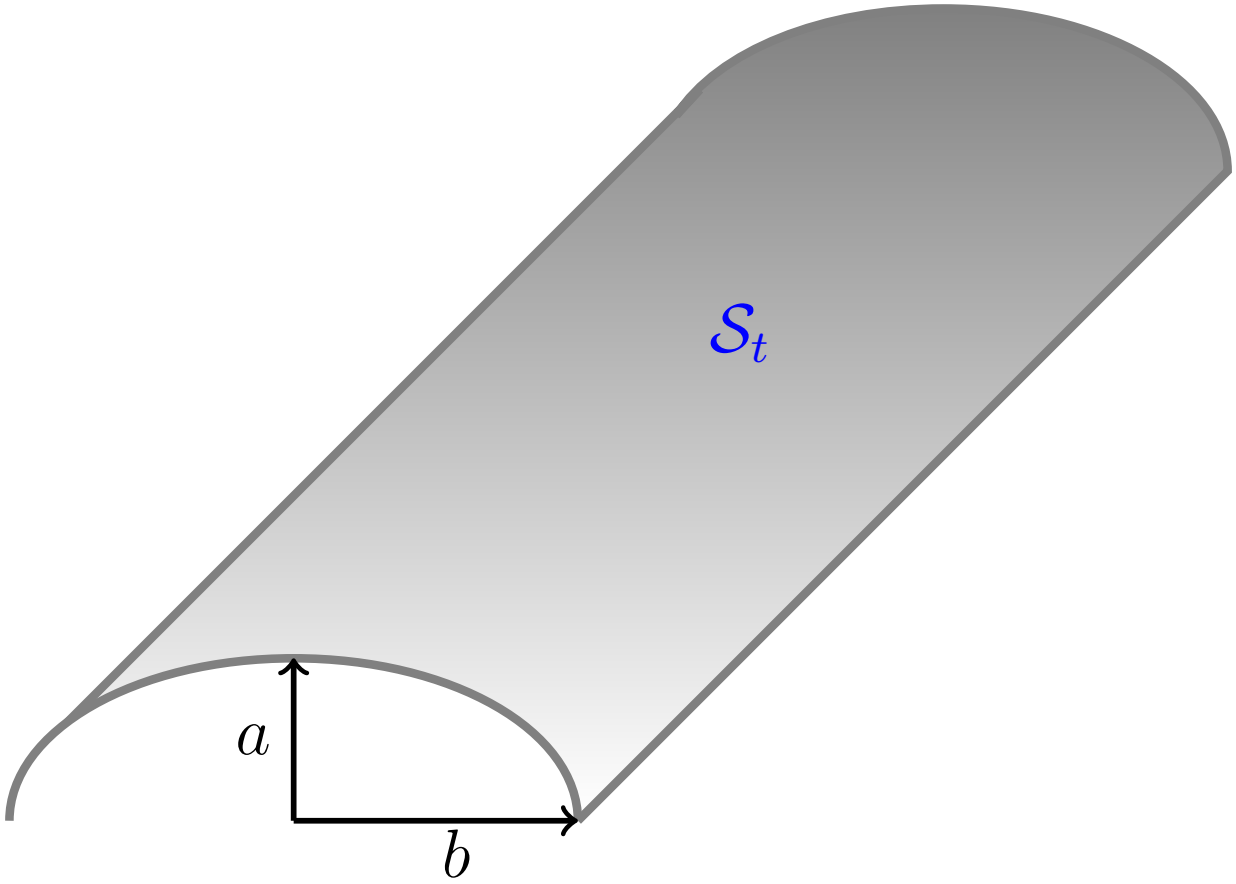

University of Sussex

Effects of curvature on pattern formation

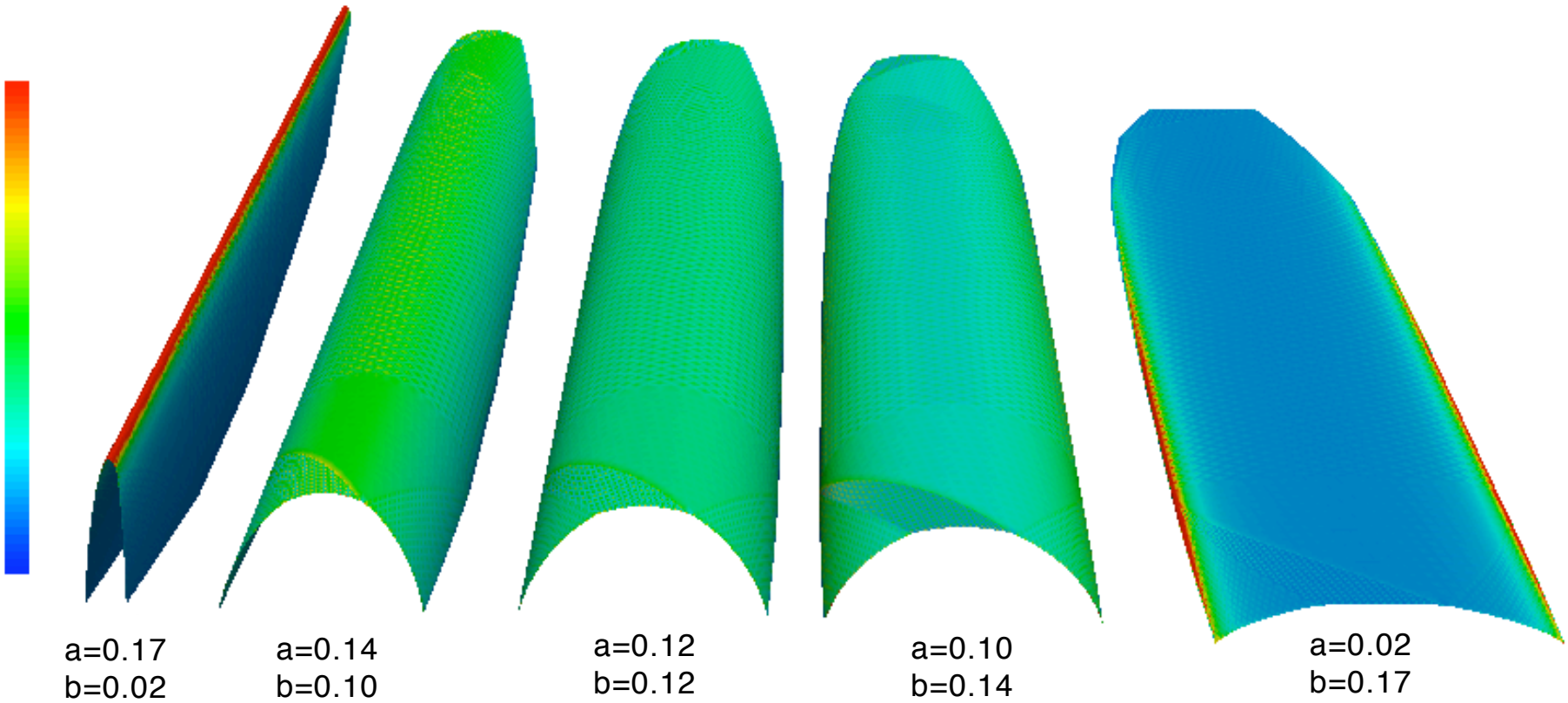

University of Sussex

Model equations

$$\begin{cases} \partial_t u_1 + \nabla_{\mathcal{S}_t} \cdot (\boldsymbol{\beta} u_1) = \nabla^2_{\mathcal{S}_t} u_1 + \gamma f_1(\boldsymbol{u}), & \\ \partial_t u_2 + \nabla_{\mathcal{S}_t} \cdot (\boldsymbol{\beta} u_2) = d\nabla^2_{\mathcal{S}_t} u_2 + \gamma f_2(\boldsymbol{u}) & \text{in } \mathcal{S}_t, (0,T], \\ \boldsymbol{u}(\boldsymbol{x},0) = \boldsymbol{u}_0(\boldsymbol{x}), & \boldsymbol{x} \in \mathcal{S}_0, \\ [\boldsymbol{\nu} \cdot \nabla_{\mathcal{S}_t} \boldsymbol{u}](\boldsymbol{x},t) = \boldsymbol{0}, & \boldsymbol{x} \in \partial\mathcal{S}_t, t > 0, \end{cases} \tag{2}$$

where d is the ratio of the diffusion coefficients, γ is a scaling parameter, $\boldsymbol{u}_0(\boldsymbol{x})$ is a well-defined positive bounded vector function. The vector $\boldsymbol{\nu}$ is the unit normal to the surface boundary $\partial\mathcal{S}_t$. The nonlinear vector valued function $\boldsymbol{f} = (f_1, f_2)^T$ represents the reaction kinetics.

University of Sussex

Thomas (1975) reaction kinetics

This is a specific substrate–inhibition reaction involving the substrates oxygen (v) and uric acid (u) which react in the presence of the enzyme uricase. The reaction kinetics, derived by fitting the kinetics to experimental data (Thomas, 1975) can be written as

$$f(u,v) = \alpha - u - \frac{\beta uv}{(1+u+kv^2)},$$

$$g(u,v) = c\kappa - cv - \frac{\beta uv}{(1+u+kv^2)},$$

where $\alpha = 92$, $\kappa = 64$, $k = 0.1$, $c = 1.5$, $\beta = 18.5$, $d = 9.75$ and $\gamma = 116$.

University of Sussex

A Lagrangian FEM for parameterisable surface

The model equations for a reaction-diffusion system (RDSs) on an evolving surface $\mathcal{S}_t$ can be written as:

$$\frac{\mathrm{d}}{\mathrm{d}t}\int_{\mathcal{S}_t} u_i \,\mathrm{d}\mathcal{S}_t = \int_{\mathcal{S}_t} D_i \nabla_{\mathcal{S}_t} \cdot (\nabla_{\mathcal{S}_t} u_i) + f_i(\boldsymbol{u}) \,\mathrm{d}\mathcal{S}_t. \tag{3}$$

We assume the surface $\mathcal{S}_t$ is parameterisable and denote by

$$\boldsymbol{\mathcal{A}} : \mathbb{R}^2 \times [0,T] \to \mathbb{R}^3, \tag{4}$$

the parameterisation. Formally we assume there exists a reference domain $\hat{\Omega} \subset \mathbb{R}^2$ such that at each instant $t \in [0,T]$ and for each $\boldsymbol{x} \in \mathcal{S}_t$ there exists a $\boldsymbol{\xi} \in \hat{\Omega}$ such that

$$\boldsymbol{\mathcal{A}}(\boldsymbol{\xi}, t) = \boldsymbol{x}. \tag{5}$$

University of Sussex

Mappings

Moreover we assume the parametrisation defined by $\boldsymbol{\mathcal{A}}$ is orthogonal, i.e.,

$$\partial_{\xi_1}\boldsymbol{\mathcal{A}} \cdot \partial_{\xi_2}\boldsymbol{\mathcal{A}} = 0 \text{ in } \hat{\Omega} \times [0, T]. \tag{6}$$

To construct a finite element method to approximate the solution of RDSs on parameterisable surfaces we need the following elementary facts from differential geometry. The *area element* of $\mathcal{S}_t$ is given by

$$\mathrm{d}\mathcal{S}_t = \partial_{\xi_1}\boldsymbol{\mathcal{A}}\partial_{\xi_2}\boldsymbol{\mathcal{A}}. \tag{7}$$

University of Sussex

Surface derivatives

Letting $\hat{u}_i(\boldsymbol{\xi}, t) = u_i\left(\boldsymbol{\mathcal{A}}(\boldsymbol{\xi}, t), t\right)$ then, since the parameterisation is orthogonal, the Laplace-Beltrami operator can be expressed on the reference frame as

$$\nabla_{\mathcal{S}_t} \cdot (\nabla_{\mathcal{S}_t} u_i) = \nabla_{\boldsymbol{\xi}} \cdot \left(\boldsymbol{G}^{-1} \nabla_{\boldsymbol{\xi}} \hat{u}_i\right), \tag{8}$$

where the matrix $\boldsymbol{G}$ is the matrix of coefficients of the *first fundamental form*:

$$\boldsymbol{G} = \begin{bmatrix} \partial_{\xi_1} \boldsymbol{\mathcal{A}}^2 & 0 \\ 0 & \partial_{\xi_2} \boldsymbol{\mathcal{A}}^2 \end{bmatrix}. \tag{9}$$

Changing variables we obtain the following expression on the reference frame

$$\frac{\mathrm{d}}{\mathrm{d}t} \int_{\hat{\Omega}} \hat{u}_i \partial_{\xi_1} \boldsymbol{\mathcal{A}} \partial_{\xi_2} \boldsymbol{\mathcal{A}} = \int_{\hat{\Omega}} \left(D_i \nabla_{\boldsymbol{\xi}} \cdot (\boldsymbol{G}^{-1} \nabla_{\boldsymbol{\xi}} u_i) + f_i(\boldsymbol{u})\right) \partial_{\xi_1} \boldsymbol{\mathcal{A}} \partial_{\xi_2} \boldsymbol{\mathcal{A}}. \tag{10}$$

US University of Sussex

Moving finite elements

We employ a Galerkin FEM for the spatial approximation and an IMEX modified backward Euler scheme for the time integration of the RDSs. For the simulations on planar domains we use a MFEM, which aims to find $U_1^n, U_2^n \in \mathbb{V}^n, n = 1, \cdots, N$ such that (Madzvamuse, 2007)

$$
\begin{cases}
\frac{1}{\tau}\langle U_1^n, \Psi^n\rangle + \langle \nabla U_1^n, \nabla \Psi^n\rangle \\
= \gamma\left\langle \alpha - U_1^n - \dfrac{\beta U_2^{n-1} U_1^n}{1 + (1 + kU_1^{n-1})U_1^{n-1}}, \Psi^n \right\rangle + \frac{1}{\tau}\langle U_1^{n-1}, \Psi^{n-1}\rangle \\
\\
\frac{1}{\tau}\langle U_2^n, \Psi^n\rangle + d\langle \nabla U_2^n, \nabla \Psi^n\rangle \\
= \gamma\left\langle c\kappa - cV_1^n - \dfrac{\beta U_1^{n-1} U_2^n}{1 + (1 + kU_1^{n-1})U_1^{n-1}}, \Psi^n \right\rangle + \frac{1}{\tau}\langle U_2^{n-1}, \Psi^{n-1}\rangle,
\end{cases}
$$

for all $\Psi^n \in \mathbb{V}^n, n = 1, \cdots, N$, where τ is the uniform timestep.

University of Sussex

ALE formulation on evolving surfaces

For the simulations on surfaces the finite element method we used aims to find $\hat{U}_1^n, \hat{U}_2^n \in \hat{\mathbb{V}}$, such that (Madzvamuse, 2007, Venkataraman et al., 2011)

$$\begin{cases} \frac{1}{\tau}\langle [J\hat{U}_1]^n - [J\hat{U}_1]^{n-1}, \hat{\Psi}\rangle & +\langle [J\boldsymbol{K}]^n \nabla \hat{U}_1^n, \boldsymbol{K}^n \nabla \hat{\Psi}\rangle \\ & = \gamma \left\langle \alpha - \hat{U}_1^n - \dfrac{\beta \hat{U}_2^{n-1}\hat{U}_1^n}{1+(1+k\hat{U}_1^{n-1})\hat{U}_1^{n-1}}, J^n\hat{\Psi} \right\rangle \\ \frac{1}{\tau}\langle [J\hat{U}_2]^n - [J\hat{U}_2]^{n-1}, \hat{\Psi}\rangle & +d\langle [J\boldsymbol{K}]^n \nabla \hat{U}_2^n, \boldsymbol{K}^n \nabla \hat{\Psi}\rangle \\ & = \gamma \left\langle c\kappa - c\hat{U}_2^n - \dfrac{\beta \hat{U}_1^{n-1}\hat{U}_2^n}{1+(1+k\hat{U}_1^{n-1})\hat{U}_1^{n-1}}, J^n\hat{\Psi} \right\rangle, \end{cases}$$

for all $\hat{\Psi} \in \hat{\mathbb{V}}$, where τ is the uniform timestep.

University of Sussex

Evolving Matrices

The matrix $\boldsymbol{K}$ and the determinant of the Jacobian J are given by

$$\boldsymbol{K} = \begin{bmatrix} \frac{1}{\partial_{\xi_1}\boldsymbol{\mathcal{A}}} & 0 \\ 0 & \frac{1}{\partial_{\xi_2}\boldsymbol{\mathcal{A}}} \end{bmatrix}, \tag{11}$$

$$\text{and} \quad J = \partial_{\xi_1}\boldsymbol{\mathcal{A}}\partial_{\xi_2}\boldsymbol{\mathcal{A}}. \tag{12}$$

In both cases the finite element spaces were made up of piecewise linear basis functions. The initial data was approximated using the Lagrange interpolant. The linear systems were solved using the conjugate gradient algorithm. In both cases we took an initial triangulation $\mathcal{T}^0$ with 6897 nodes and a fixed timestep of 10^{-2}.

University of Sussex

Approximate activator concentration on planar domains

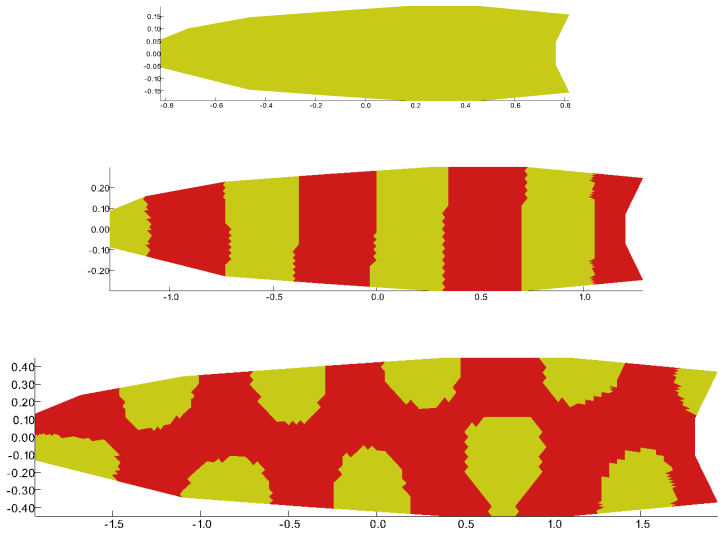

University of Sussex

Approximate activator concentration on planar domains

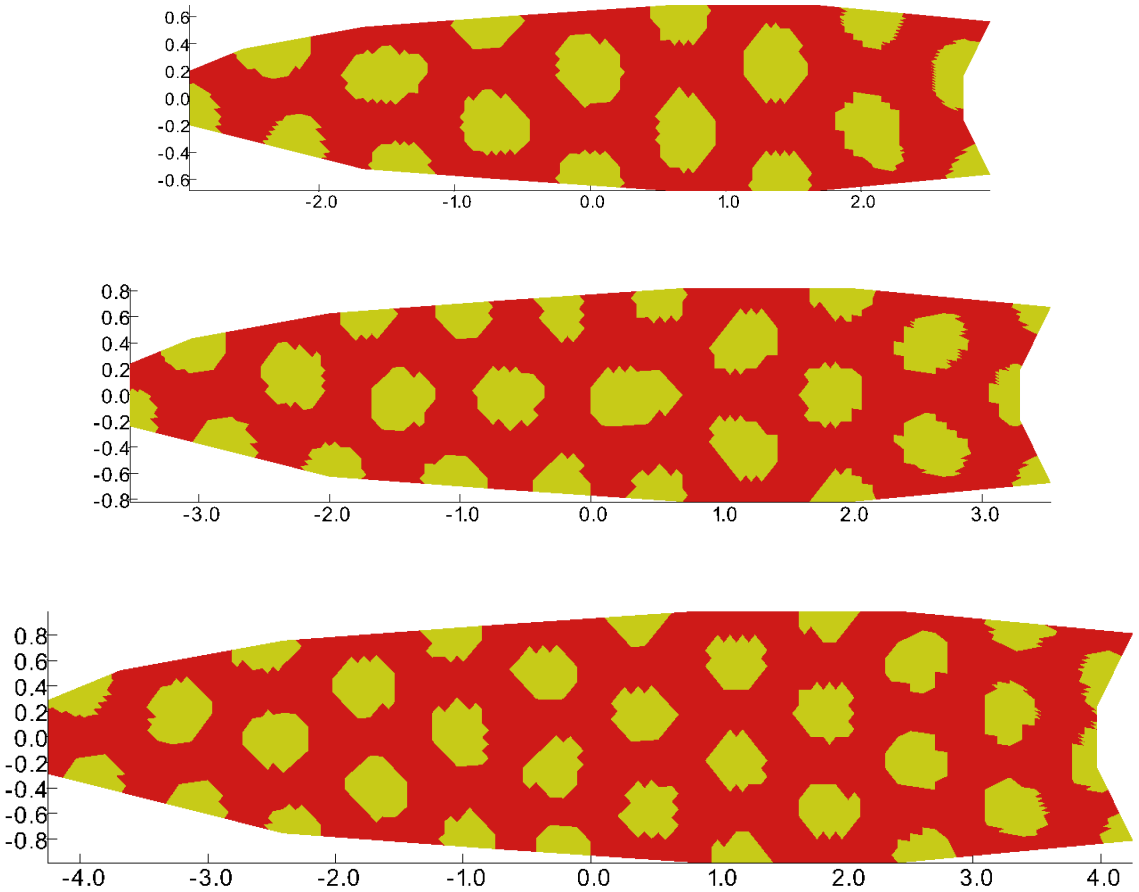

University of Sussex

Approximate activator concentration on cylinders

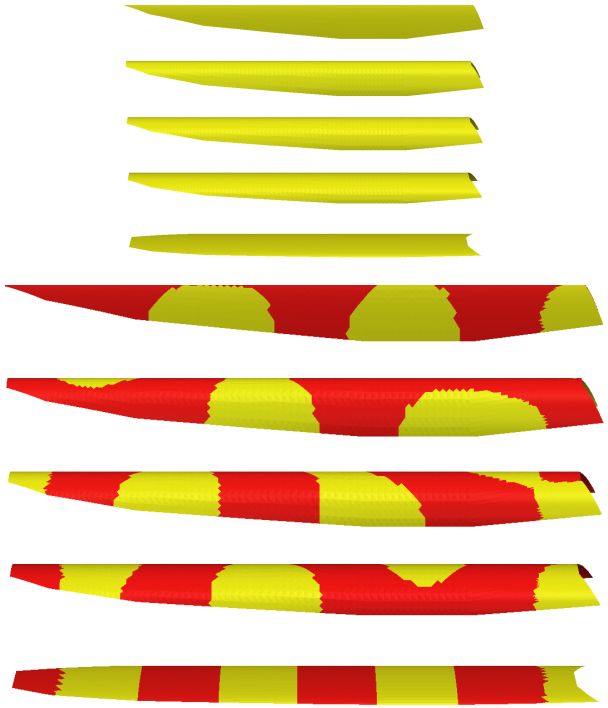

University of Sussex

Approximate activator concentration on cylinders

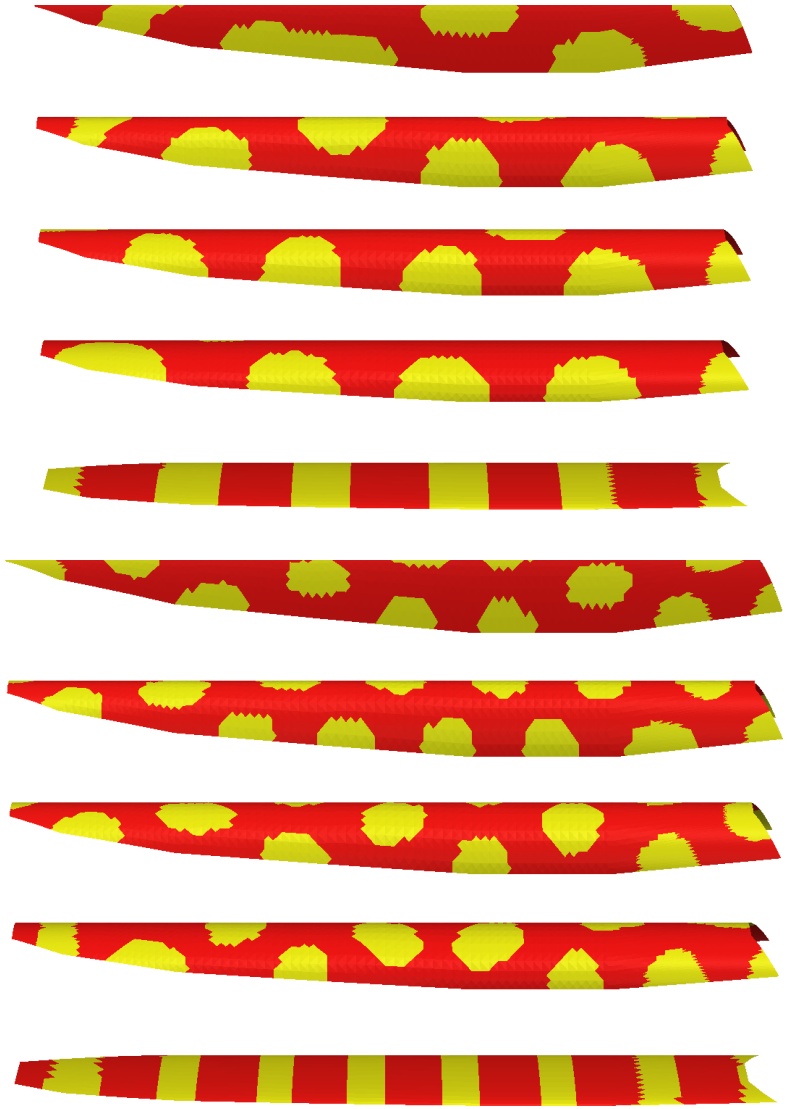

University of Sussex

Approximate activator concentration on cylinders

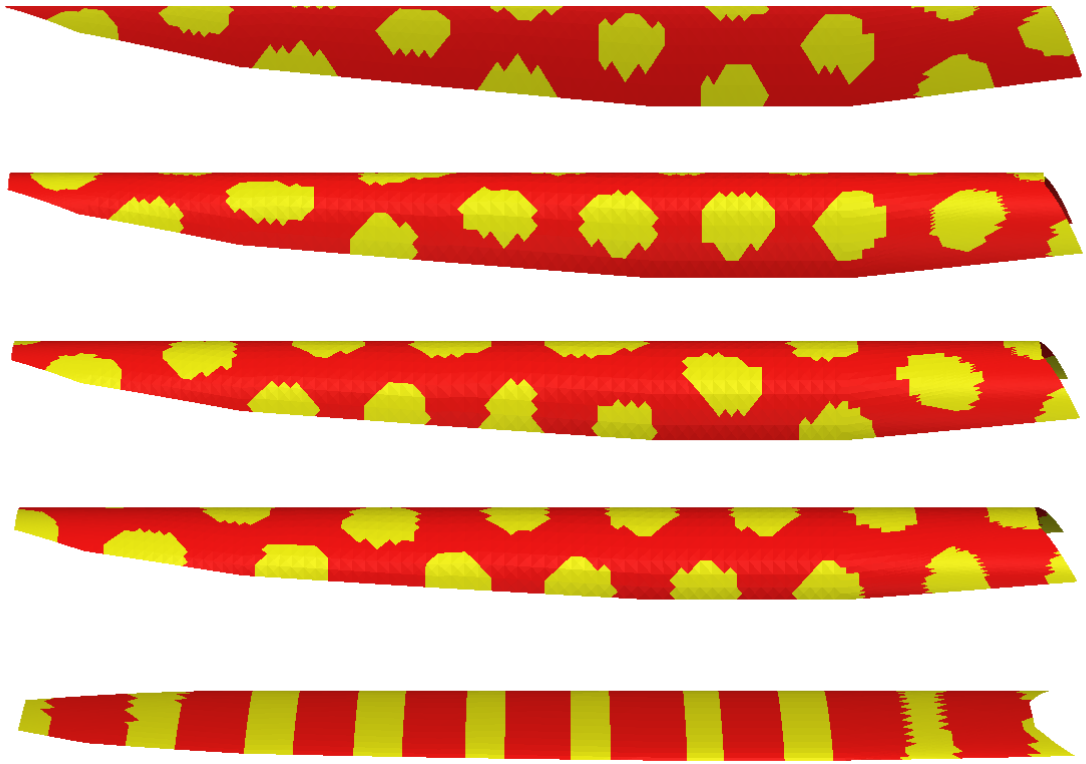

University of Sussex

Approximate activator concentration on cylinders

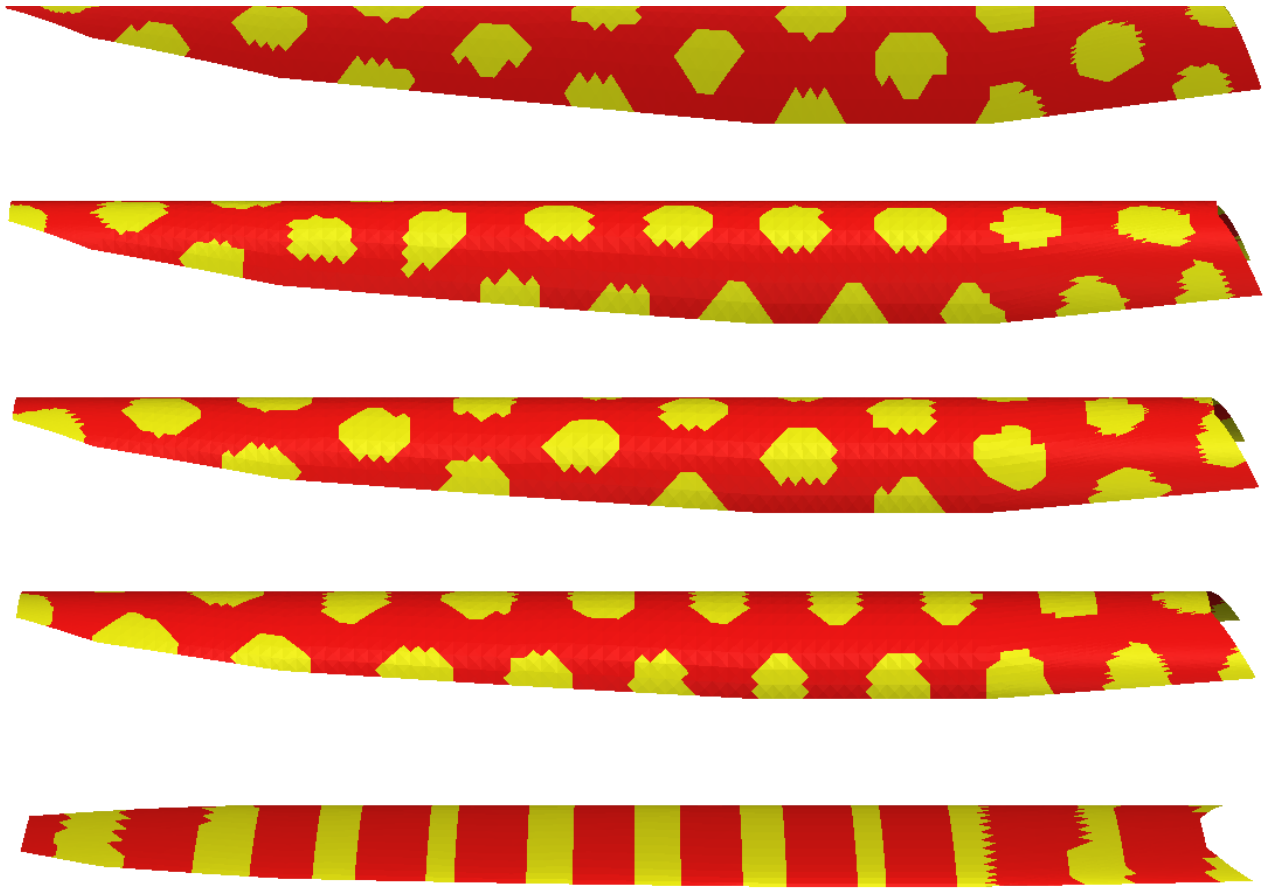

University of Sussex

Take home message!

- Understanding the role of domain growth is critical in the Life Sciences
- Pose models (PDEs) on arbitrary evolving surfaces
- Numerically solve highly complex nonlinear PDES on evolving surfaces (ESFEM, RPFEM)
- Tackle problems in Life Sciences involving growth development

University of Sussex

Current research articles

- Barreira, R. Elliott, C.M. & Madzvamuse, A. (2011). *The surface finite element method for pattern formation on evolving biological surfaces*. Journal of Mathematical Biology. Online
- Chandrashekar, V. Sekimura T. Eamonn, G.A. Maini, P.K. & Madzvamuse, A. (2011). *A model for parr mark pattern formation during the early development of Amago trout*. Physica Rev. E. Online.
- Tuncer, N. Meir, A.J. & Madzvamuse, A. (2012). *Radially projected finite elements for reaction-diffusion Systems on fixed spheroidal domains*. In preparation.
- Tuncer, N. Meir, A.J. & Madzvamuse, A. (2012). *Radially projected finite elements for reaction-diffusion Systems on evolving spheroidal domains*. In preparation.
- Madzvamuse, A. (2007). *A modified backward Euler scheme for advection-reaction-diffusion systems.* Mathematical Modeling of Biological Systems, Volume I. A. Deutsch, L. Brusch, H. Byrne, G. de Vries and H.-P. Herzel (eds). Birkhuser, Boston, 191-197.
- Madzvamuse A. (2006). *Time-stepping schemes for moving grid finite elements applied to reaction-diffusion systems on fixed and growing domains*. J. of Comp. Phys. 214, 239-263.

University of Sussex

Acknowledgements: Funding

- EPSRC grant: *Mathematical modelling of spatial patterning on evolving surfaces*
- The British Council: UK-US Travel Grant: *Prime Minister's Initiative for International Education (PMI2)*
- NSF: Masamu Programme - Memorandum of Understanding with Auburn.

University of Sussex